



Identification of four novel mutations in *VSP13A* in Iranian patients with Chorea-acanthocytosis (ChAc)

Vadieh Ghodsinezhad¹ · Abdoreza Ghoreishi² · Mohammad Rohani³ · Mahdi Dadfar⁴ · Akbar Mohammadzadeh⁵ · Ali Rostami⁶ · Hamzeh Rahimi^{7,8}

Received: 7 September 2023 / Accepted: 13 January 2024
© The Author(s), under exclusive licence to Springer-Verlag GmbH Germany, part of Springer Nature 2024

Abstract

Chorea-acanthocytosis (ChAc) is a rare autosomal recessive neurodegenerative disorder characterized by a variety of involuntary movements, predominantly chorea, and the presence of acanthocytosis in peripheral blood smears. ChAc is caused by mutations in the vacuolar protein sorting-associated protein 13A (*VPS13A*) gene. The aim of the present study was to conduct a clinical and genetic analysis of five patients with suspected ChAc in Iran. This study included five patients who were referred to the genetic department of the Endocrinology and Metabolism Research Institute between 2020 and 2022, with a suspicion of ChAc. Clinical features and the presence of characteristic MRI findings were evaluated in the patients. Whole-exome sequencing (WES) followed by Sanger sequencing was employed to identify the disease-causing variants. The functional effects of novel mutations were analyzed by specific bioinformatics prediction tools. WES and data analysis revealed the presence of five distinct *VPS13A* mutations in the patients, four of which were novel. These included one non-sense mutation (p.L984X), and three splice site mutations (c.755-1G>A, c.144+1 G>C, c.2512+1G>A). All mutations were validated by Sanger sequencing, and in silico analysis predicted that all mutations were pathogenic. This study provides the first molecular genetic characteristics of Iranian patients with ChAc, identifying four novel mutations in the *VPS13A* gene. These findings expand the *VPS13A* variants spectrum and confirm the clinical variability in ChAc patients.

Keywords Chorea-acanthocytosis (ChAc) · *VPS13A* · Whole-exome sequencing (WES) · Mutation · Neuroimaging · In silico

Communicated by Shuhua Xu.

✉ Ali Rostami
rostami@zums.ac.ir

✉ Hamzeh Rahimi
hrahimi@txbiomed.org

Vadieh Ghodsinezhad
Vadieh95@gmail.com

Abdoreza Ghoreishi
ar.ghoreishy@gmail.com

Mohammad Rohani
mohammadroohani@gmail.com

Mahdi Dadfar
mahdidadfar1989@gmail.com

Akbar Mohammadzadeh
akbarmohammadzadeh1348@gmail.com

² Department of Neurology, Faculty of Medicine, Zanzan University of Medical Sciences, Zanzan, Iran

³ Department of Neurology, Rasoul Akram Hospital, School of Medicine, Iran University of Medical Sciences, Tehran, Iran

⁴ Skull Base Research Center, Rasoul Akram Hospital, Iran University of Medical Sciences, Tehran, Iran

⁵ Department of Genetics and Molecular Medicine, Faculty of Medicine, Zanzan University of Medical Sciences, Zanzan, Iran

⁶ Department of Pharmacology, Faculty of Medicine, Zanzan University of Medical Sciences, Zanzan, Iran

⁷ Department of Molecular Medicine, Biotechnology Research Center, Pasteur Institute of Iran, Tehran, Iran

⁸ Texas Biomedical Research Institute, San Antonio, TX, USA

¹ Department of Genetics and Molecular Medicine, Faculty of Medicine, Zanzan University of Medical Sciences, Zanzan, Iran

Introduction

Chorea-acanthocytosis (ChAc, MIM 200150) or VPS13A disease is a rare autosomal recessive inherited syndrome that was first described by Critchley et al. in 1967 (Critchley et al. 1967; Walker and Danek 2021). ChAc is a neuroacanthocytosis syndrome (NA) that also includes McLeod syndrome (MLS, MIM#300842), Huntington's disease-like 2 (HDL2, MIM#606438) and pantothenate kinase-associated neurodegeneration (PKAN, MIM#606157) (Walker 2015; Benninger et al. 2016). It is characterized by adult-onset, hyperkinetic involuntary movements, specifically chorea, and orofacial dyskinesia. Patients have variable clinical symptoms, including peripheral neuropathy, seizure, dystonia, parkinsonism, tics, elevated serum creatine kinase (CK), and peripheral blood acanthocytes (Walker 2015; Walker et al. 2007; Tomiyasu et al. 2011). The main neuropathological feature of ChAc is atrophy of the striatum, including the caudate nucleus (Walker et al. 2007; Shen et al. 2017).

The causative gene, vacuolar protein sorting 13 homolog A (*VPS13A*, OMIM: *65978), is a compound of 73 exons, spanning 250 kb on chromosome 9q21, and encodes a 360-kDa protein also named chorein (Rampoldi et al. 2001). Chorein is an endoplasmic reticulum-anchored protein belonging to the VPS13 family of lipid transporters. Recent studies have demonstrated that chorein and lipid scramblase XK are functional partners at the plasma membrane (Kurano et al. 2007; Park et al. 2022). Chorein regulates many vital processes, including cytoskeletal architecture, calcium homeostasis, autophagy, and cell survival (Dziurdzik and Conibear 2021; Dobson-Stone et al. 2004).

VPS13A gene mutations usually lead to markedly reduced levels or the absence of chorein in the tissues of ChAc patients (Rampoldi et al. 2001; Dobson-Stone et al. 2004). The final diagnosis of ChAc can be made by either protein expression analysis or DNA sequencing of the *VPS13A* gene (Huang et al. 2022; Vaisfeld et al. 2021). To date, 166 mutations have been reported in *VPS13A* in the Human Gene Mutation Database (HGMD) (<http://www.hgmd.cf.ac.uk/ac/index.php>). Genetic investigation using the direct Sanger sequencing technique is complicated due to the large size of the gene (250 kb) and the lack of mutation hotspots (Ouchkat et al. 2020; Dulski et al. 2016). Next-generation sequencing (NGS) is a cost-effective and time-saving genetic diagnosis of ChAc patients.

The prevalence of ChAc is estimated to be approximately 1:1,000,000 cases worldwide (Jung et al. 2011; Nishida et al. 2019). ChAc has been reported in different countries, including China, Japan, Germany, the United States, and Iran (Shen et al. 2017; Yi et al. 2018; Weber

et al 2019). ChAc is more prevalent in Japan due to the presence of a founder effect. More than 100 ChAc patients have been reported in this country (Jung et al. 2011).

In Iran, only a few cases of ChAc have been reported, and most of them were diagnosed based on clinical symptoms without genetic testing (Karkheiran et al. 2012; Ghabeli-Juibary and Rezaeitalab 2016). Here, we studied five cases of suspected ChAc based on clinical symptoms and neuroimaging features. In addition, we utilized Whole-exome sequencing (WES) to identify the disease-causing variants.

Methods

Ethics statements

This research was conducted in accordance with the principles of the Declaration of Helsinki. The Bioethics Committee of Zanjan University of Medical Sciences (ZUMS) approved this study (IR.ZUMS.REC.1398.345). Written informed consent was obtained from the patients and their parents for participation in the study.

Patients and clinical evaluations

Five Iranian patients suspected of having ChAc according to clinical and neurological findings were included in this study. All patients had typical features of ChAc, including hyperkinetic movements, elevated creatine kinase levels, and acanthocytes in peripheral blood smears. Brain magnetic resonance imaging (MRI) of all five patients showed bilateral caudate atrophy and putaminal hyperintensity on T2/FLAIR sequences. The patient's clinical details are summarized in Table 1. All patients were born to healthy consanguineous parents. The family histories of all patients did not show similar conditions except for the last case, which had a sister with similar symptoms but with less severity. Blood samples from the patients and their parents were taken after obtaining informed consent.

Whole-exome sequencing (WES)

Genomic DNA was extracted from the peripheral blood lymphocytes of patients and their parents by standard methods. DNA samples from patients were subjected to WES. Exome capture and library preparation were performed using the Agilent SureSelectV7kit (Agilent Technologies, Santa Clara, CA, USA) according to the manufacturer's protocols. WES was performed by the Illumina HiSeq6000 platform (Illumina, San Diego, CA, USA). The sequencing reads were mapped to the hg19/b37 reference human genome using the Burrows–Wheeler Aligner (BWA) tool. The variant calling process was run using the Genome Analysis Toolkit

Table 1 Summary of clinical and laboratory findings in ChAc patients

Patient No	1	2	3	4	5
Gender	Male	Male	Male	Male	Male
Age	39	29	35	36	42
Age of Onset	33	16	22	33	34
Consanguinity	+	+	+	+	+
Family history	–	–	–	–	+
First symptoms	Gait disturbance	Tics	Chorea	Generalized tonic–clonic seizures	Seizures
Chorea	+	+	+	+	+
Dystonia	+	+	+	+	+
Orofacial dyskinesia	+	–	–	+	+
Tongue and lip biting	+	–	–	+	+
Parkinsonian features	+	–	+	–	+
Electromyography (EMG)	Not available	Polymyopathy	Not available	Axonal sensory-motor polyneuropathy	Axonal sensory-motor polyneuropathy
Seizure	–	–	–	+	+
Dysphagia	+	–	+	+	+
Dysarthria	+	–	+	+	+
Neuropsychiatric symptoms	+	–	+	+	+
Neuroimaging (MRI)	Bilateral caudate atrophy and hyperintensity of caudate and putamens	Bilateral caudate atrophy and hyperintensity of caudate and putamens	Bilateral caudate atrophy and hyperintensity of caudate and putamens	Bilateral caudate atrophy and hyperintensity of caudate and putamens	Bilateral caudate atrophy and hyperintensity of caudate and putamens
Acanthocytes	+	+	+	+	+
Creatine Kinase (U/L)	1700	2500	1500	1230	3900

(GATK), and then variants were annotated with ANNOVAR software.

Allele frequency was assessed using several databases, including the 1000 Genomes Project (<http://www.1000genomes.org/>), dbSNP (<http://www.ncbi.nlm.nih.gov/projects/SNP/>), Exome Sequencing Project (ESP, 6500 exomes, <http://evs.gs.washington.edu/EVS/>), Genome Aggregation Database (gnomAD), and Exome Aggregation Consortium (ExAC, Cambridge, MA, <http://exac.broadinstitute.org/>). Reported pathogenicity was assessed by consulting disease databases such as ClinVar (<http://www.ncbi.nlm.nih.gov/clinvar/>) and the Human Gene Mutation Database (HGMD, (<http://www.hgmd.cf.ac.uk>)). The identified variants were classified according to the American College of Medical Genetics and Genomics (ACMG) guidelines from 2015. To predict the effect of missense variants, various bioinformatics tools were used, such as SIFT, PolyPhen-2, PROVEAN, MutationTaster, and Combined Annotation Dependent Depletion (CADD).

Variant confirmation by Sanger sequencing

The corresponding exons of all candidate variants were PCR amplified and sequenced by the Sanger method in the patients

and their parents. Primers were designed using the Primer3 algorithm and purchased from Gen Fan Avaran Company.

The primer sequences and PCR conditions are listed in Supplementary Tables S1 and S2, respectively. The Sanger sequencing results were compared with the reference sequence (NM_033305.3) of *VPS13A* via NCBI BLAST software.

In silico prediction of splicing mutations

Several In silico splice site prediction programs, including NNSPLICE0.9 (https://www.fruitfly.org/seq_tools/splice.html), ASSP (<http://wangcomputing.com/assp/>), and NetGene2 (<http://www.cbs.dtu.dk/services/NetGene2/>), were used to predict the functional effects of novel splice site variants.

Results

Clinical findings

Patient 1 is a 39-year-old man who developed gait disturbance as the first symptom at the age of 33 years. His

symptoms progressed, and orofacial dyskinesias, lip and tongue biting and parkinsonism were added to the clinical features. On neurologic examination, he had dysarthria, a masked face, hypokinesia, and rigidity of limbs. Deep tendon reflexes (DTRs) were absent. Eye movements and fundoscopic examination were normal. He had mild choreiform in the oromandibular area, eating dystonia, and dystonic gait. Sensory and cerebellar examinations were normal. Brain MRI revealed bilateral caudate atrophy and caudate and putaminal hyperintensity on T2/FLAIR sequences (Fig. 1A). Acanthocytes were detected on peripheral blood smear, and serum creatine kinase was elevated (1700 U/L).

Patient 2 is a 29-year-old man who was referred with initial symptoms of tics beginning at the age of 16, followed by dystonia and generalized chorea. Laboratory tests showed remarkably elevated serum CK levels (2500 U/L) and acanthocytosis on the peripheral blood smear. Brain MRI showed hyperintensity of the striatum (caudate and putamen) on T2/FLAIR sequences with bilateral caudate atrophy (Fig. 1B). Electromyography revealed polymyopathy.

Patient 3 is a 35-year-old male who presented with chorea. His symptoms started with chorea and gradually

evolved to dystonia. On neurologic examination, he had dysarthria, severe generalized choreiform movement, recurrent head and neck backward deviation, eating dystonia, and dystonic gait. He also had generalized areflexia. Eye movements were normal. The brain MRI was similar to previous cases. Laboratory work-up showed acanthocytes on the peripheral blood smear and elevated serum CK levels (1500 U/L).

Patient 4 The first symptom of this 36-year-old male started at the age of 33 with a generalized tonic-clonic seizure. Later, he developed difficulty in eating, abnormal movements in his hands, and gait disturbance. On the first examination, he had mild dysarthria, normal eye movements, and mild choreiform movements in the oromandibular area and hands. On follow-up examinations, chorea worsened in all limbs and the face, and he had severe eating dystonia, which led to an eating disorder and weight loss. Muscle stretch reflexes were unobtainable. EMG demonstrated axonal sensory-motor polyneuropathy. The brain MRI was similar to previous cases. High levels of CK (1230 U/L) were detected in the serum, and acanthocytes were found on the peripheral blood smear (Fig. 1C).

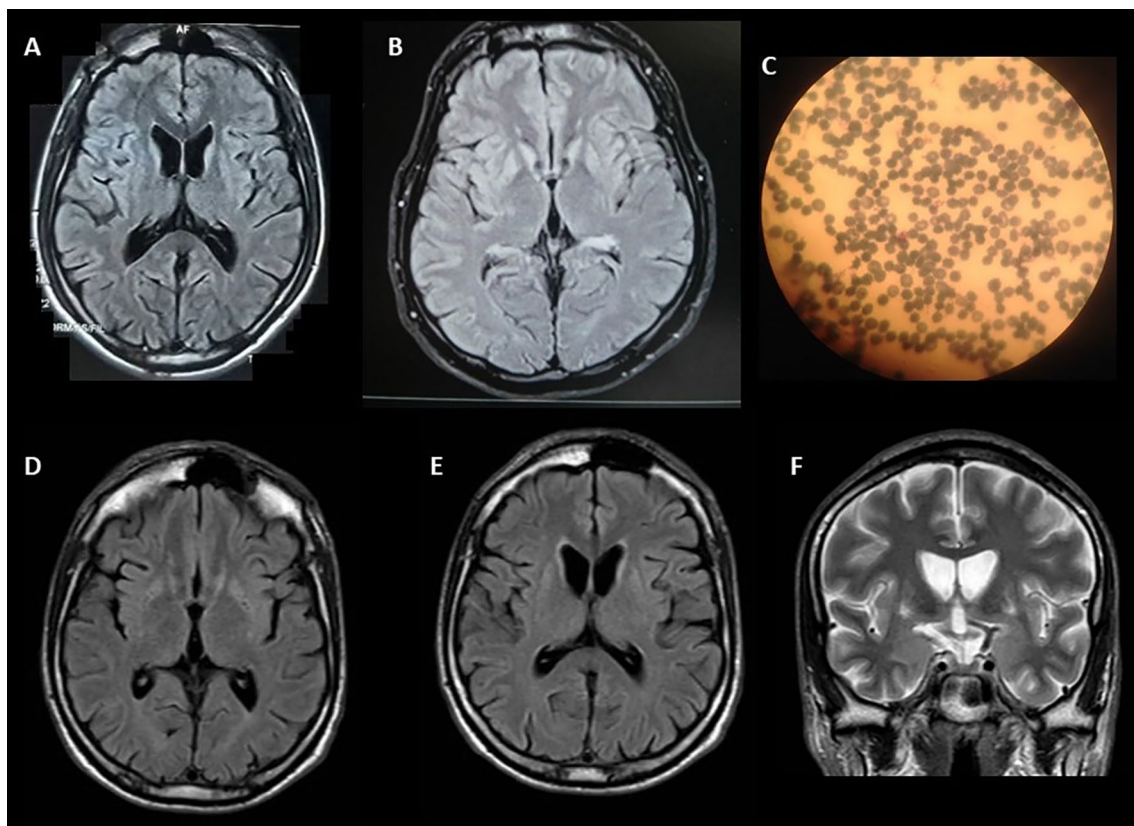


Fig. 1 Neuroimaging and biological features of ChAc patients in the current study. The axial brain MRI of patient 1 (T2/FLAIR sequence) shows caudate atrophy and hyperintensity (A). Brain MRI revealed caudate atrophy and hyperintensity on axial T2/FLAIR sequence in

patient 2 (B). Peripheral blood smear of patient 4 with acanthocytosis (C). Brain MRI of patient 5 showing caudate atrophy and hyperintensity on axial T2/FLAIR (D and E) and coronal T2 sequences (F)

Patient 5 is a 42-year-old male who came to our attention with phonic tics, eating dystonia, dysarthria and, as a first symptom, seizures that started at the age of 34 years. On examination, he had phonic tics and choreiform movements in the neck, arms, legs, and trunk with recurrent truncal and neck retrobending. Gait was impaired due to mixed chorea and dystonia. Eye movements were normal. Deep tendon reflexes were unobtainable. His younger sister had similar problems with seizures as the initial presentation and a milder form of chorea. Brain MRI revealed caudate atrophy and hyperintensity on axial T2/FLAIR and coronal T2 sequences (Fig. 1D–F). Laboratory tests showed acanthocytosis and a considerable elevation in serum CK (3900 U/L). EMG revealed axonal sensory-motor polyneuropathy.

Whole-exome sequencing and Sanger confirmation

The bioinformatics analysis of WES data revealed that all five patients had a homozygous mutation in *VPS13A*, as shown in Table 2. Sanger sequencing confirmed all of the identified *VPS13A* mutations (Fig. 2A–E).

Patient 1 had a previously reported homozygous nonsense mutation (c.C5881T, p.R1961*) in exon 45 of *VPS13A*, leading to a premature stop codon. The homozygous mutation detected by WES was confirmed in the patient using Sanger sequencing, and his parents had heterozygous alleles.

In *patient 2*, WES identified a homozygous variant c.755-1G>A in the canonical splice acceptor site of exon 11 of *VPS13A*. The homozygous c.755-1G>A variant was confirmed in the patient by Sanger sequencing. His parents were both heterozygous for the c.755-1G>A variant. In *Patient 3*, WES data analysis revealed a homozygous variant c.144+1 G>C in the canonical splice donor site of exon 2 of *VPS13A*. This variant was confirmed by Sanger sequencing, and both parents were heterozygous carriers of the c.144+1 G>C variant.

Patient 4 had a homozygous nonsense variant c.2951T>A (p.L984*) in exon 28 of *VPS13A*, predicted to lead to premature truncation of the protein at codon 984 (Table 2). This nonsense variant was confirmed in the patient using Sanger sequencing. Both parents were heterozygous for the p.L984* variant. Finally, *patient 5* had a homozygous variant c.2512+1G>A, located in the canonical splice donor site of exon 24 of *VPS13A*. The patient's parents were heterozygous carriers for the c.2512+1G>A variant.

As shown in Table 2, among the 5 variants identified in the present study, only c.5881C>T (in patient 1) was previously reported as a disease-causing mutation (Ogawa et al. 2013). The other 4 variants were not found in any disease databases, such as HGMD and ClinVar. Moreover, these variants were not detected in control databases such as the 1000G, EVS, ExAC, and dbSNP or in the literature. Additionally, these variants were absent in the Iranome database.

In silico analysis

Table 3 presents the results of the In silico analysis of novel splice site variants using the NNSplice, ASSP, and Netgene2 tools.

For *patient 2*, the variant c.755-1G>A was predicted by ASSP, NNSplice, and Netgene2 to disrupt the normal acceptor splice site (tcattttttattttttcAGtatttcgcccattatctgct). These programs identified an alternative splice acceptor site (ctttaattttcattctttAGtatttcagttattatggagct) located at the 3' end of intron 11, with scores of 8.395 (ASSP), 0.96 (NNSplice), and 0.27 (Netgene2). This alteration is expected to result in the skipping of exon 11, leading to a frameshift and the formation of a premature termination codon (Fig. 3A).

In the case of *patient 3*, the variant c.144+1G>C was predicted by ASSP, NNSplice, and Netgene2 to affect the wild-type donor splice site (tgcctgGTaggttt) at the end of

Table 2 *VPS13A* mutations found in the present study and related information

Patient No	1	2	3	4	5
cDNA Variant (NM_033305.3)	c.5881C>T	c.755-1G>A	c.144+1 G>C	c.2951T>A	c.2512+1G>A
Variant Type	Nonsense	Splice-site Acceptor Substitution	Splice-site Donor Substitution	Nonsense	Splice-site Acceptor Substitution
Protein change	p.R1961*	Unknown	Unknown	p.L984*	Unknown
Exon Number	45	11	2	28	24
Zygosity	Hom	Hom	Hom	Hom	Hom
Frequency in public Databases (ExAC, 1000G, EVS, Iranome)	NR	NR	NR	NR	NR
CADD	44	24	25.6	36	25.9
Reported (HGMD, ClinVar)	Ogawa et al. (2013) (CM135837)	NR	NR	NR	NR

ExAC Exome Aggregation Consortium, 1000G 1000 Genomes Project, EVS Exome Variant Server, CADD Combined Annotation Dependent Depletion, NR Not reported, Hom Homozygote

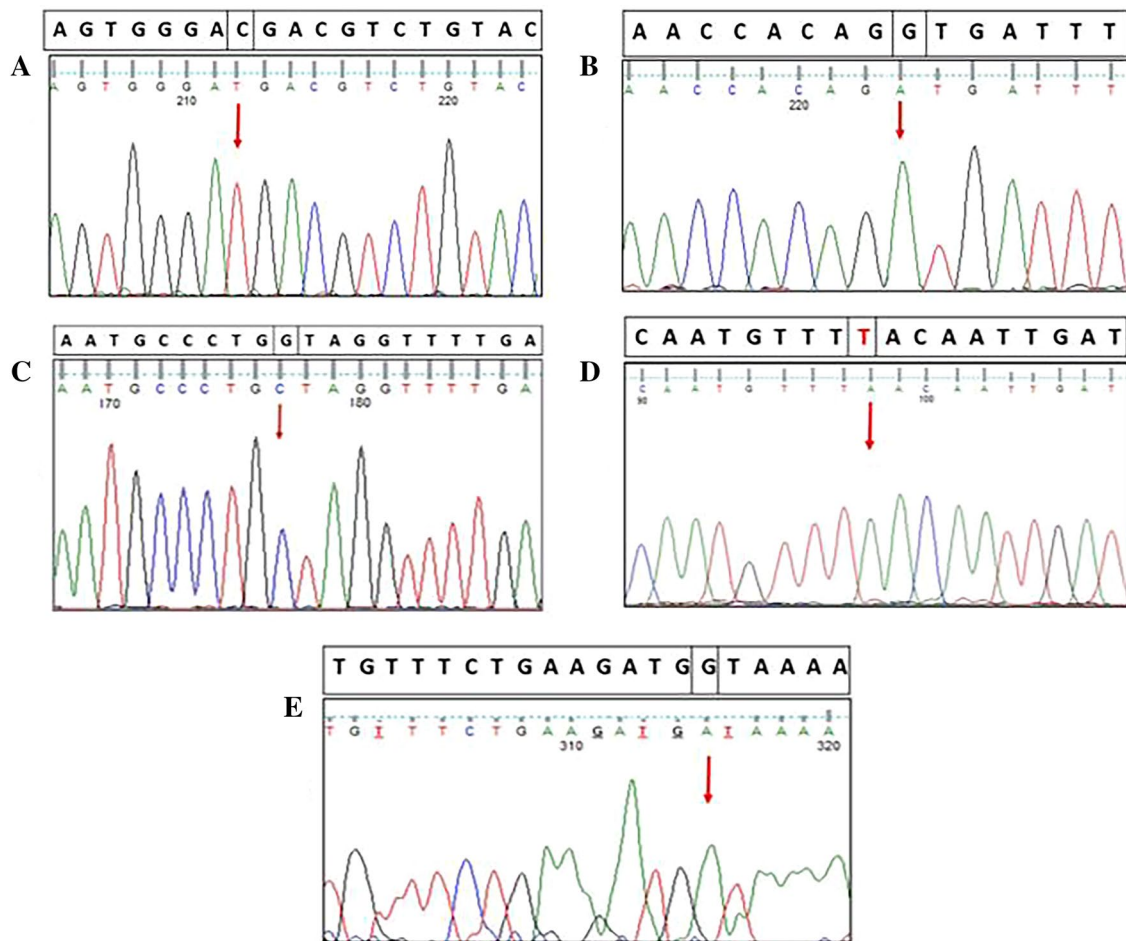


Fig. 2 Sanger sequencing chromatograms of the DNA genomic region encompassing the *VPS13A* mutations in our patients. **A** Patient 1: The homozygous mutation c.5881C>T (p.R1961X) in exon 45. **B** Patient 2: The homozygous mutation c.755-1G>A in exon 11.

C Patient 3: The homozygous mutation c.144+1 G>C in exon 2. **D** Patient 4: The homozygous mutation c.2951T>A (p.L984X) in exon 28. **E** Patient 5: The homozygous mutation c.2512+1G>A in exon 24. The red arrow indicates the mutation site

Table 3 In silico prediction analysis of novel splice site mutations in our patients

In silico Prediction tools		ASSP Score*		NNSplice Score**		Netgene2 Confidence***	
		WT	MUT	WT	MUT	WT	MUT
Patient 2	c.755-1G>A Acceptor Site	8.926	8.395	0.96	0.96	0.20	0.27
Patient 3	c.144+1 G>C Donor Site	9.530	8.225	0.72	0.57	0.80	ND
Patient 5	c.2512+1G>A Donor Site	8.142	6.171	0.65	0.52	0.42	0.34

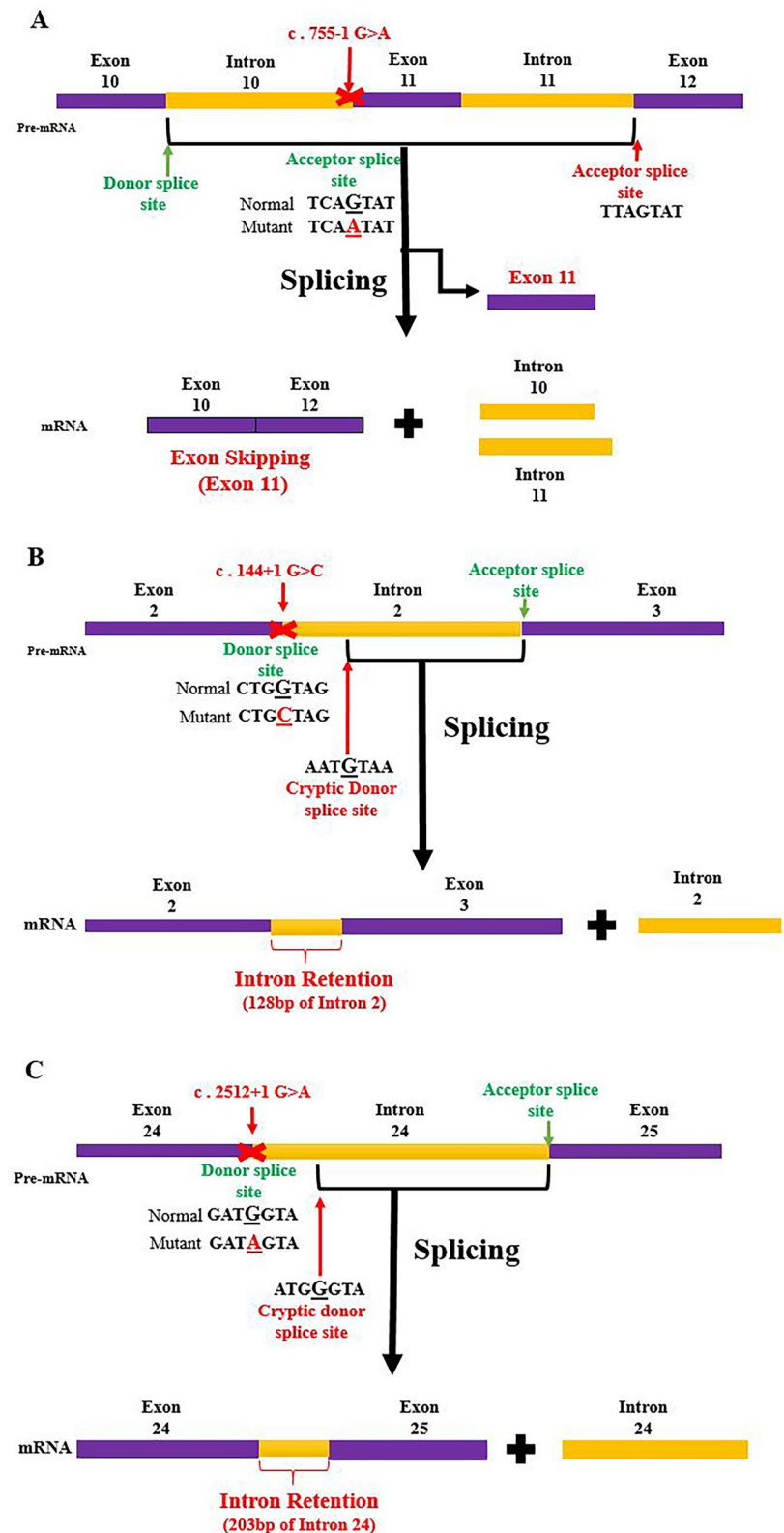
WT wild-type, MUT mutant, ND Not detected

*ASSP: Acceptor splice-site cutoff: 2.2, Donor splice-site cutoff: 4.5

**NNSplice: Acceptor splice-site score cutoff: 0.40, Donor splice-site score cutoff: 0.40

***Netgene2: Acceptor splice-site confidence cutoff: 20%, Donor splice-site confidence cutoff: 50%

Fig. 3 Ideogram of predicted consequences of the splice-site mutations on *VPS13A* mRNA. **A** The c.755-1G>A mutation disrupts the normal acceptor splice site and is predicted to cause a frameshift due to the skipping of exon 11. **B** The c.144+1 G>C mutation in patient 3 destroys the normal splice donor site and is predicted to be the inclusion of part of intron 2 (128bp intron retention). **C** The c.2512+1G>A mutation in patient 5 disrupts the normal donor splice site and is predicted to cause a frameshift due to the 203 bp retention of intron 24. The natural splice site positions are marked in green, while the mutation sites and new splice sites are marked in red



exon 2. ASSP and NNSplice identified a cryptic donor site at position c.144+127 (gcaaaatGTaaatt) within intron 2, with scores of 8.225 and 0.57, respectively. This cryptic

donor splice site may lead to the retention of 128 bp of intron 2 and, consequently, the occurrence of a premature stop codon (Fig. 3B). However, NetGene2 did not detect any cryptic splice sites in this case.

For *patient 5*, the variant c.2512+1G>A was predicted by ASSP, NNSplice, and Netgene2 to disrupt the wild-type donor splice site (gaagatgGTaaaatg) at the end of exon 24. Both ASSP and NNSplice further predicted a cryptic splice site (ttcatggGTacatgc) within intron 24 at position c.2512+202. The corresponding scores assigned by ASSP and NNSplice to this cryptic splice site were 6.171 and 0.52, respectively. This alteration is likely to result in a frameshift due to the retention of 203 bp of intron 24, leading to the formation of a premature termination codon (Fig. 3C). However, NetGene2 identified c.2512+331 (gggaggcaagG-Tatatggga) as a potential donor site with a score of 0.34 but did not recognize c.2512+202 as a significant splice site.

Discussion

Herein, we present a study of five suspected ChAc cases according to clinical symptoms and neuroimaging features, which were further genetically confirmed. ChAc usually manifests between ages 20 and 40 and rarely below age 20 or after 50 (Walker et al. 2007). The median age of our patients was 36.2 years (range 29–42), and the mean age at onset was 27.6 years (range 16–34). Laboratory investigations revealed increased serum CK levels and acanthocytes in blood smears of all five patients. Indeed, elevated serum CK is a very useful indicator and can be seen in most ChAc patients, in contrast to acanthocytosis, which is not a consistent finding (Huang et al. 2022; Spieler et al. 2020). On the other hand, atrophy of the caudate nucleus is a typical finding in brain MRIs of ChAc patients (Huang et al. 2022; Weber et al. 2019; Connolly et al. 2014). This was confirmed in the present study, as brain MRI of all our patients showed variable degrees of caudate atrophy and putamen hyperintensity on T2/FLAIR sequences.

The first symptoms of our patients were gait disturbances (patient 1), tics (patient 2), chorea (patient 3), and seizures (patients 4 and 5). According to the literature, while a distinct feature of NA syndromes is chorea, other movement disorders have also been reported, including dystonia, parkinsonism, and tics (Dulski et al. 2016; Zhu et al. 2019). However, it should be noted that chorea appeared as a presenting symptom in all our patients in the later stages of the disease. Orofacial dyskinesia of varied severity develops in most patients with NA syndromes (Critchley et al. 1967; Dulski et al. 2016). Several reports have shown that tongue and lip biting are suggestive indicators of ChAc (Shen et al. 2017; Huang et al. 2022; Dulski et al. 2016; Rubio et al. 1997). In our study, tongue and lip biting were present in three patients (patients 1, 4, and 5).

Recent studies have revealed that epilepsy is a crucial presentation in ChAc patients, and 42% of patients have a history of epileptic seizures (Benninger et al. 2016; Weber

et al. 2019; Luo et al. 2021). Indeed, in our study, seizures were present and were observed as the first symptoms in 2 patients (4 and 5) out of 5 (40%). It has been suggested that *VPS13A* mutations may affect the interaction of this gene with the phosphoinositide 3-kinase gene (PI3K) and lead to epilepsy by disrupting calcium signals in neurons. Although we noticed in our study and in the literature that approximately 40% of the ChAc patients presented epilepsy, there is no clear evidence as to why some patients show epilepsy while others do not (Luo et al. 2021; Steinlein 2014).

In ChAc, neurophysiologic studies may suggest a predominantly axonal neuropathy and myopathy (Walker et al. 2007; Vance et al. 1987). In our study, electromyography revealed evidence of axonal sensory-motor polyneuropathy (patients 4 and 5) and polymyopathy (patient 2). As already documented in the literature and in our study, high clinical variability was seen among ChAc patients, and there was no genotype–phenotype correlation (Walker 2015; Jung et al. 2011; Ouchkat et al. 2020; Dulski et al. 2016).

All five of our ChAc patients had a homozygous mutation in the *VPS13A* gene. They included two nonsense mutations (p.R1961X and p.L984X in patients 1 and 4, respectively) and three splice-site mutations (c.755-1G>A, c.144+1 G>C, and c.2512+1G>A in patients 2, 3 and 5, respectively). Only one of the *VPS13A* mutations in our patients (p.R1961* in patient 1) was reported previously in ChAc patients (Table 2 and Fig. 4). Ogawa et al. reported the p.R1961* mutation in two Japanese siblings with ophthalmologic involvement, although our patient had no relevant symptoms. It remains unclear whether eye involvement in their patients is specifically attributed to this mutation (Ogawa et al. 2013).

The other four mutations found in our patients were apparently novel mutations and had not been published so far. Three novel splice-site mutations were predicted to affect mRNA translation by either skipping the adjacent exon (Patient 2) or misreading the affected intron (patients 3 and 5). In silico analysis by ASSP, NNSplice, and Netgene2 predicted these mutations to be likely pathogenic. Since the cDNA samples from our patients were not accessible, we could not evaluate the precise effects of these novel mutations. Overall, these findings suggest potential consequences for splice site mutations in patients 2, 3, and 5. Further studies are needed to confirm these predictions and assess their impact on protein function.

Considering the autosomal recessive inheritance of the disease and the high rate of consanguineous marriages in Iran, it is likely that the number of affected individuals is higher. However, the prevalence of ChAc in Iran is not well-established due to the limited number of case reports. In 2012, Karkheiran et al. described the first three Iranian patients with a clinical diagnosis of ChAc, which was confirmed through a chorein Western blot assay (Karkheiran et al. 2012). Later, Ghabeli et al. reported a ChAc patient

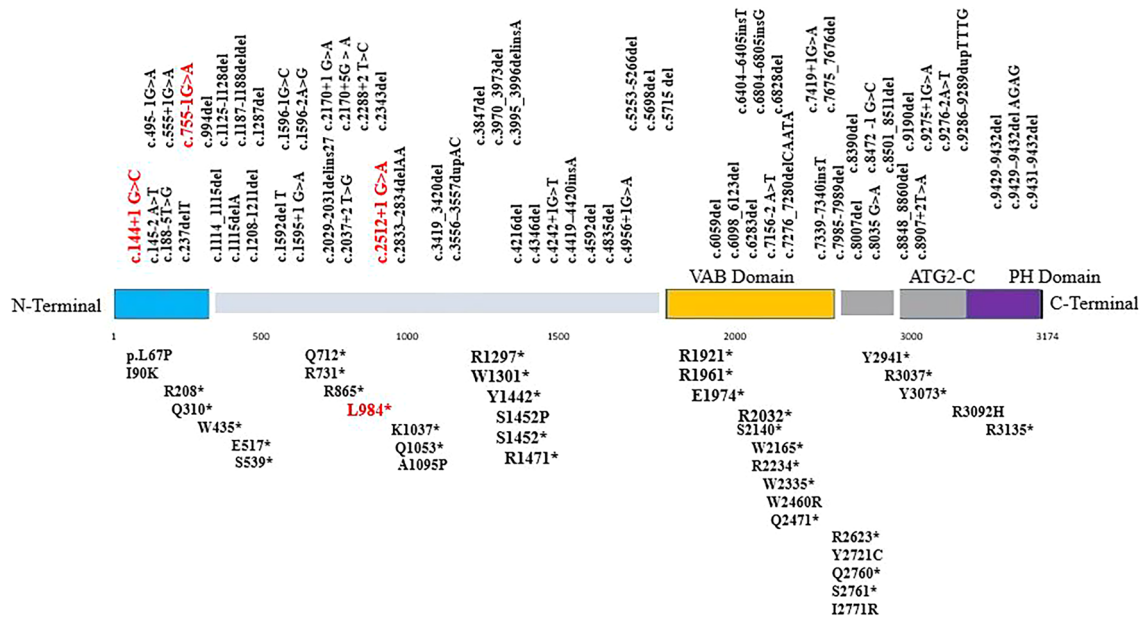


Fig. 4 Schematic representation of the VPS13A protein domain structure and the positions of mutations reported for ChAc in the HGMD Database. Small deletions/insertions and splicing mutations are located above the diagram, while nonsense/missense mutations are positioned below. The novel mutations identified in this study are

who was diagnosed based on characteristic clinical features and peripheral acanthocytosis, but genetic confirmation was not obtained (Ghabeli-Juibary and Rezaeitalab 2016). In this study, we identified four novel and one previously reported *VPS13A* mutations in five Iranian ChAc patients, using whole-exome sequencing. To our knowledge, this is the first study reporting genetically diagnosed ChAc patients in Iran.

Conclusion

In conclusion, all five patients with a clinical diagnosis of ChAc were found to be homozygous for a mutation in *VPS13A*. Therefore, the diagnosis of ChAc in these patients was genetically confirmed. Our findings demonstrate an expanded mutational spectrum of *VPS13A* through four novel mutations.

Supplementary Information The online version contains supplementary material available at <https://doi.org/10.1007/s00438-024-02111-y>.

Acknowledgements In memory of Omid Aryani for his deep understanding of neurology, great interest in education, and science friendship. The authors wish to express their deepest gratitude to the patients and their families that participated in this study.

Author contributions AR, AM, and AGh: contributed to study conception and design. MR and MD collected clinical data. VGh and HR performed the experiments and analyzed and interpreted the data. AR and

HR supervised the study. VGh, MR, and MD: drafted the manuscript and designed the figures. All authors contributed to the final manuscript and approved the submitted version.

Funding This work was extracted from the Ph.D degree thesis of Vadih Ghodsinezhad, supported by the deputy of research of Zanjan University of Medical Sciences, Zanjan, Iran (Grant No: A-12-167-4).

Data availability All data generated during and/or analyzed during the current study are available upon request from the corresponding authors. All novel mutations identified in the study have been submitted to the ClinVar database. The ClinVar accession numbers for the identified mutations are as follows: SCV004030267 (c.144+1G>C), SCV004030268 (c.755-1G>A), SCV004030269 (c.2512+1G>A), and SCV004030270 (c.2951T>A).

Declarations The authors have no relevant financial or non-financial interests to disclose.

References

Conflict of interests The authors have no relevant financial or non-financial interests to disclose.

References

- Benninger F, Afawi Z, Korczy AD, Oliver KL, Pendziwiat M, Nakamura M, Sano A, Helbig I, Berkovic SF, Blatt I (2016) Seizures as presenting and prominent symptom in chorea-acanthocytosis with c.2343del *VPS13A* gene mutation. *Epilepsia* 57(4):549–556. <https://doi.org/10.1111/epi.13318>
- Connolly BS, Hazrati LN, Lang AE (2014) Neuropathological findings in chorea-acanthocytosis: new insights into mechanisms

- underlying parkinsonism and seizures. *Acta Neuropathol* 127(4):613–615. <https://doi.org/10.1007/s00401-013-1241-3>
- Critchley EM, Clark DB, Wikler A (1967) an adult form of acanthocytosis. *Trans Am Neurol Assoc* 92:132–137. <https://doi.org/10.1001/archneur.1968.00470320036004>
- Dobson-Stone C, Velayos-Baeza A, Filippone LA, Westbury S, Storch A, Erdmann T, Wroe SJ, Leenders KL, Lang AE, Dotti MT, Federico A, Mohiddin SA, Fananapazir L, Daniels G, Danek A, Monaco AP (2004) Chorein detection for the diagnosis of chorea-acanthocytosis. *Ann Neurol* 56(2):299–302. <https://doi.org/10.1002/ana.20200>
- Dulski J, Sołtan W, Schinwelski M, Rudzińska M, Wójcik-Pędzwiatr M, Wictor L, Schön F, Puschmann A, Klempf J, Tilley L, Roth J, Tacik P, Fujioka S, Drozdowski W, Sitek EJ, Wszolek Z, Sławek J (2016) Clinical variability of neuroacanthocytosis syndromes—a series of six patients with long follow-up. *Clin Neurol Neurosurg* 147:78–83. <https://doi.org/10.1016/j.clineuro.2016.05.028>
- Dziurdzik SK, Conibear E (2021) The Vps13 family of lipid transporters and its role at membrane contact sites. *Int J Mol Sci* 22(6):2905. <https://doi.org/10.3390/ijms22062905>
- Ghabeli-Juibary A, Rezaeitalab F (2016) Neuroacanthocytosis in two brothers: an ultra-rare cause of movement disorder. *Caspian J Neurol Sci* 2(2):50–53. <https://doi.org/10.18869/acadpub.cjns.2.5.50>
- Guillén-Samander A, Wu Y, Pineda SS, García FJ, Eisen JN, Leonzino M, Ugur B, Kellis M, Heiman M, De Camilli P (2022) A partnership between the lipid scramblase XK and the lipid transfer protein VPS13A at the plasma membrane. *Proc Natl Acad Sci USA* 119(35):e2205425119. <https://doi.org/10.1073/pnas.2205425119>
- Huang S, Zhang J, Tao M, Lv Y, Xu L, Liang Z (2022) Two case reports of chorea-acanthocytosis and review of literature. *Eur J Med Res* 27(1):22. <https://doi.org/10.1186/s40001-022-00646-7>
- Jung HH, Danek A, Walker RH (2011) Neuroacanthocytosis syndromes. *Orphanet J Rare Dis* 6:68. <https://doi.org/10.1186/1750-1172-6-68>
- Karkheiran S, Bader B, Roohani M, Danek A, Shahidi GA (2012) Chorea-acanthocytosis: report of three cases from Iran. *Arch Iran Med* 15(12):780–782
- Kurano Y, Nakamura M, Ichiba M, Matsuda M, Mizuno E, Kato M, Agemura A, Izumo S, Sano A (2007) In vivo distribution and localization of chorein. *Biochem Biophys Res Commun* 353(2):431–435. <https://doi.org/10.1016/j.bbrc.2006.12.059>
- Luo FM, Deng MX, Yu R, Liu L, Fan LL (2021) Case report: chorea-acanthocytosis presents as epilepsy in a consanguineous family with a nonsense mutation of in VPS13A. *Front Neurosci* 15:604715. <https://doi.org/10.3389/fnins.2021.604715>
- Nishida Y, Nakamura M, Urata Y, Kasamo K, Hiwatashi H, Yokoyama I, Mizobuchi M, Sakurai K, Osaki Y, Morita Y, Watanabe M, Yoshida K, Yamane K, Miyakoshi N, Okiyama R, Ueda T, Wakasugi N, Saitoh Y, Sakamoto T, Takahashi Y et al (2019) Novel pathogenic VPS13A gene mutations in Japanese patients with chorea-acanthocytosis. *Neurol Genet* 5(3):e332. <https://doi.org/10.1212/NXG.0000000000000332>
- Ogawa I, Saigoh K, Hirano M, Mtsui Y, Sugioka K, Takahashi J, Shimomura Y, Tani Y, Nakamura Y, Kusunoki S (2013) Ophthalmologic involvement in Japanese siblings with chorea-acanthocytosis caused by a novel chorein mutation. *Parkinsonism Relat Disord* 19(10):913–915. <https://doi.org/10.1016/j.parkreldis.2013.05.012>
- Ouchkat F, Regragui W, Smaili I, Naciri Darai H, Bouslam N, Rahmani M, Melhaoui A, Arkha Y, El Fahime E, Bouhouche A (2020) Novel pathogenic VPS13A mutation in Moroccan family with Choreoacanthocytosis: a case report. *BMC Med Genet* 21(1):47. <https://doi.org/10.1186/s12881-020-0983-8>
- Park JS, Hu Y, Hollingsworth NM, Miltenberger-Miltenyi G, Neiman AM (2022) Interaction between VPS13A and the XK scramblase is important for VPS13A function in humans. *J Cell Sci* 135(17):jcs260227. <https://doi.org/10.1242/jcs.260227>
- Rampoldi L, Dobson-Stone C, Rubio JP, Danek A, Chalmers RM, Wood NW, Verellen C, Ferrer X, Malandrini A, Fabrizi GM, Brown R, Vance J, Pericak-Vance M, Rudolf G, Carrè S, Alonso E, Manfredi M, Németh AH, Monaco AP (2001) A conserved sorting-associated protein is mutant in chorea-acanthocytosis. *Nat Genet* 28(2):119–120. <https://doi.org/10.1038/88821>
- Rubio JP, Danek A, Stone C, Chalmers R, Wood N, Verellen C, Ferrer X, Malandrini A, Fabrizi GM, Manfredi M, Vance J, Pericak-Vance M, Brown R, Rudolf G, Picard F, Alonso E, Brin M, Németh AH, Farrall M, Monaco AP (1997) Chorea-acanthocytosis: genetic linkage to chromosome 9q21. *Am J Hum Genet* 61(4):899–908. <https://doi.org/10.1086/514876>
- Shen Y, Liu X, Long X, Han C, Wan F, Fan W, Guo X, Ma K, Guo S, Wang L, Xia Y, Liu L, Huang J, Lin Z, Xiong N, Wang T (2017) Novel VPS13A gene mutations identified in patients diagnosed with chorea-acanthocytosis (ChAc): case presentation and literature review. *Front Aging Neurosci* 9:95. <https://doi.org/10.3389/fnagi.2017.00095>
- Spieler D, Velayos-Baeza A, Mühlbäck A, Castrop F, Maegerlein C, Slotta-Huspenina J, Bader B, Haslinger B, Danek A (2020) Identification of two compound heterozygous VPS13A large deletions in chorea-acanthocytosis only by protein and quantitative DNA analysis. *Mol Genet Genomic Med* 8(9):e1179. <https://doi.org/10.1002/mgg3.1179>
- Steinlein OK (2014) Calcium signaling and epilepsy. *Cell Tissue Res* 357(2):385–393. <https://doi.org/10.1007/s00441-014-1849-1>
- Tomiyasu A, Nakamura M, Ichiba M, Ueno S, Saiki S, Morimoto M, Kobal J, Kageyama Y, Inui T, Wakabayashi K, Yamada T, Kanemori Y, Jung HH, Tanaka H, Orimo S, Afawi Z, Blatt I, Aasly J, Ujike H, Babovic-Vuksanovic D, Josephs KA, Tohge R, Rodrigues GR, Dupré N, Yamada H, Yokochi F, Kotschet K, Takei T, Rudzińska M, Szczudlik A, Penco S, Fujiwara M, Tojo K, Sano A (2011) Novel pathogenic mutations and copy number variations in the VPS13A gene in patients with chorea-acanthocytosis. *Am J Med Genet B Neuropsychiatr Genet* 156B:620–631. <https://doi.org/10.1002/ajmg.b.31206>
- Vaisfeld A, Bruno G, Petracca M, Bentivoglio AR, Servidei S, Vita MG, Bove F, Straccia G, Dato C, Di Iorio G, Sampaolo S, Peluso S, De Rosa A, De Michele G, Barghigiani M, Galatolo D, Tessa A, Santorelli F, Chiurazzi P, Melone MAB (2021) Neuroacanthocytosis syndromes in an Italian cohort: clinical spectrum, high genetic variability and muscle involvement. *Genes* 12(3):344. <https://doi.org/10.3390/genes12030344>
- Vance JM, Pericak-Vance MA, Bowman MH, Payne CS, Fredane L, Siddique T, Roses AD, Massey EW (1987) Chorea-acanthocytosis: a report of three new families and implications for genetic counselling. *Am J Med Genet* 28(2):403–410. <https://doi.org/10.1002/ajmg.1320280219>
- Walker RH (2015) Untangling the thorns: advances in the neuroacanthocytosis syndromes. *J Movement Disord* 8(2):41–54. <https://doi.org/10.14802/jmd.15009>
- Walker RH, Danek A (2021) “Neuroacanthocytosis”—overdue for a taxonomic update. *Tremor Other Hyperkinetic Movements (new York, N Y)*. <https://doi.org/10.5334/tohm.583>
- Walker RH, Jung HH, Dobson-Stone C, Rampoldi L, Sano A, Tison F, Danek A (2007) Neurologic phenotypes associated with acanthocytosis. *Neurology* 68(2):92–98. <https://doi.org/10.1212/01.wnl.0000250356.78092.cc>
- Walker RH, Schulz VP, Tikhonova IR, Mahajan MC, Mane S, Arroyo Muniz M, Gallagher PG (2012) Genetic diagnosis of neuroacanthocytosis disorders using exome sequencing. *Movement Disord* 27(4):539–543. <https://doi.org/10.1002/mds.24020>
- Weber J, Frings L, Rijntjes M, Urbach H, Fischer J, Weiller C, Meyer PT, Klebe S (2019) Chorea-acanthocytosis presenting as

- autosomal recessive epilepsy in a family with a novel VPS13A mutation. *Front Neurol* 9:1168. <https://doi.org/10.3389/fneur.2018.01168>
- Yi F, Li W, Xie N, Zhou Y, Xu H, Sun Q, Zhou L (2018) Chorea-acanthocytosis in a chinese family with a pseudo-dominant inheritance mode. *Front Neurol* 9:594. <https://doi.org/10.3389/fneur.2018.00594>
- Zhu H, Feng XM, Zhao T, Liu JY (2019) Neuroacanthocytosis with unusual clinical features: a case report. *Medicine* 98(2):e14050. <https://doi.org/10.1097/MD.00000000000014050>

Publisher's Note Springer Nature remains neutral with regard to jurisdictional claims in published maps and institutional affiliations.

Springer Nature or its licensor (e.g. a society or other partner) holds exclusive rights to this article under a publishing agreement with the author(s) or other rightsholder(s); author self-archiving of the accepted manuscript version of this article is solely governed by the terms of such publishing agreement and applicable law.

Terms and Conditions

Springer Nature journal content, brought to you courtesy of Springer Nature Customer Service Center GmbH (“Springer Nature”).

Springer Nature supports a reasonable amount of sharing of research papers by authors, subscribers and authorised users (“Users”), for small-scale personal, non-commercial use provided that all copyright, trade and service marks and other proprietary notices are maintained. By accessing, sharing, receiving or otherwise using the Springer Nature journal content you agree to these terms of use (“Terms”). For these purposes, Springer Nature considers academic use (by researchers and students) to be non-commercial.

These Terms are supplementary and will apply in addition to any applicable website terms and conditions, a relevant site licence or a personal subscription. These Terms will prevail over any conflict or ambiguity with regards to the relevant terms, a site licence or a personal subscription (to the extent of the conflict or ambiguity only). For Creative Commons-licensed articles, the terms of the Creative Commons license used will apply.

We collect and use personal data to provide access to the Springer Nature journal content. We may also use these personal data internally within ResearchGate and Springer Nature and as agreed share it, in an anonymised way, for purposes of tracking, analysis and reporting. We will not otherwise disclose your personal data outside the ResearchGate or the Springer Nature group of companies unless we have your permission as detailed in the Privacy Policy.

While Users may use the Springer Nature journal content for small scale, personal non-commercial use, it is important to note that Users may not:

1. use such content for the purpose of providing other users with access on a regular or large scale basis or as a means to circumvent access control;
2. use such content where to do so would be considered a criminal or statutory offence in any jurisdiction, or gives rise to civil liability, or is otherwise unlawful;
3. falsely or misleadingly imply or suggest endorsement, approval, sponsorship, or association unless explicitly agreed to by Springer Nature in writing;
4. use bots or other automated methods to access the content or redirect messages
5. override any security feature or exclusionary protocol; or
6. share the content in order to create substitute for Springer Nature products or services or a systematic database of Springer Nature journal content.

In line with the restriction against commercial use, Springer Nature does not permit the creation of a product or service that creates revenue, royalties, rent or income from our content or its inclusion as part of a paid for service or for other commercial gain. Springer Nature journal content cannot be used for inter-library loans and librarians may not upload Springer Nature journal content on a large scale into their, or any other, institutional repository.

These terms of use are reviewed regularly and may be amended at any time. Springer Nature is not obligated to publish any information or content on this website and may remove it or features or functionality at our sole discretion, at any time with or without notice. Springer Nature may revoke this licence to you at any time and remove access to any copies of the Springer Nature journal content which have been saved.

To the fullest extent permitted by law, Springer Nature makes no warranties, representations or guarantees to Users, either express or implied with respect to the Springer nature journal content and all parties disclaim and waive any implied warranties or warranties imposed by law, including merchantability or fitness for any particular purpose.

Please note that these rights do not automatically extend to content, data or other material published by Springer Nature that may be licensed from third parties.

If you would like to use or distribute our Springer Nature journal content to a wider audience or on a regular basis or in any other manner not expressly permitted by these Terms, please contact Springer Nature at

onlineservice@springernature.com